ISSN: 2230-9926

Available online at http://www.journalijdr.com

IJDR

International Journal of Development Research
Vol. 4, Issue, 3, pp. 672-677, March, 2014

International Journal of
DEVELOPMENT RESEARCH

Full Length Research Article

DESIGN OF SINGLE-INPUT FUZZY LOGIC CONTROL OF FLYBACK MULTI-OUTPUT QUASI RESONANT CONVERTER

***Anitha, T. and Arulselvi, S.**

Department of E & I, Annamalai University, Annamalai Nagar, India

ARTICLE INFO

Article History:
Received 08th January, 2014
Received in revised form
11th February, 2014
Accepted 15th February, 2014
Published online 14th March, 2014

Key words:
Dc-dc converters,
Flyback converter,
Fuzzy logic control ,
Single input fuzzy logic control.

ABSTRACT

Power supply voltages in digital systems have been reduced considerably in recent years and often digital components requiring different voltages are present in the same board. This has increased the demand for multiple output power distribution systems with tight load regulation. In this paper, a detailed analysis and design of a multi-output fly back zero voltage switching (ZVS) quasi resonant converter (QRC) has been carried out. In order to improve the performances of the converter due to nonlinearity, intelligent controller like conventional fuzzy logic controller and single input fuzzy logic controller are proposed and simulated. The output results for load regulations are presented and the performances of both the controllers are compared. The result reveals that single input fuzzy logic controller gives satisfactory performances.

INTRODUCTION

Multi-output PWM dc-dc converters are widely used in communications, aerospace and computer systems, as they are usually more compact and less expensive than a collection of single-output converters. Fig. 1 shows the schematic of single power converter with multiple outputs, e.g. flyback converter with multiple secondary windings, and regulates one output. This leads to poor load regulation in the others outputs. In some cases each output is regulated by feedback control and others tracks as best they can. This scheme is known as cross regulation. In aerospace applications the allowable size and weight are highly restricted to accommodate greater payload. In the effort to increase the power density of power supplies, the switching frequency is pushed to high values which, in PWM converter realizations, normally lead to considerable power loss. Another significant drawback of the switch-mode operation is the EMI produced due to large di/dt and dv/dt. To overcome these short comings, new families of QRCs are introduced (Baha, 1999; Issa Batarseh, 2004; Dananjayan *et al*., 1998). The design and control of multi-output forward FM-ZCS-QRC is presented (Baha, 1999). The detailed analysis and technique of determining the cross regulation characteristics of a two-output half-bridge clamped series resonant converter (SRC) operating in the discontinuous conduction mode below resonance are reported (Jai P. Agarwal, 2000). This topology requires a wide range of frequency band in order to regulate disturbances the output voltage against load variations and supply disturbances. To eliminate this constant frequency (CF)-ZVS-QRC is proposed (Arulselvi *et al*., 2005). It has two switches, the presence of the auxiliary switch provide inductor freewheeling thereby reducing the control range of frequencies when compared with the conventional FM-QRCs. The converter may thus be called a CF-ZVS-QRC. This paper presents the design and simulation of a closed loop control using conventional fuzzy logic controller and single input fuzzy logic controller for the multi-output flyback ZVS-QRC. All simulation works are carried out using MATLAB/SIMULINK software. The performances of two control techniques are compared.

Corresponding author: Anitha, T.
Department of E & I, Annamalai University, Annamalai Nagar, India

Analysis of Multi-Ouput Flyback ZVS-QRC

The circuit diagram of multi-output flyback ZVS-QRC is shown in the Fig. 2. The switch S_1 is the main switch. The elements L_r and C_r form the resonant tank circuit. By adding an auxiliary switch S_2 in parallel with the resonant inductor L_r, the switching frequency band required to regulate the output voltage for a given load change is reduced. The auxiliary switch S_2 is used to control the off time of the switching period. Here, the converter is operated in half-wave mode. The

elements L_m, L_1 and L_2 represent the primary, secondary1 and secondary2 inductances, respectively. The current through the primary of the transformer is assumed as magnetizing current I_m, which is equal to i_{Lr}. The following parameters are defined (Issa Batarseh, 2004; Arulselvi *et al*., 2005) for the analysis: Characteristics impedance=Z_0, resonant angular frequency =ω_0, resonant frequency = f_0, resonant capacitor voltage = V_{cr}.

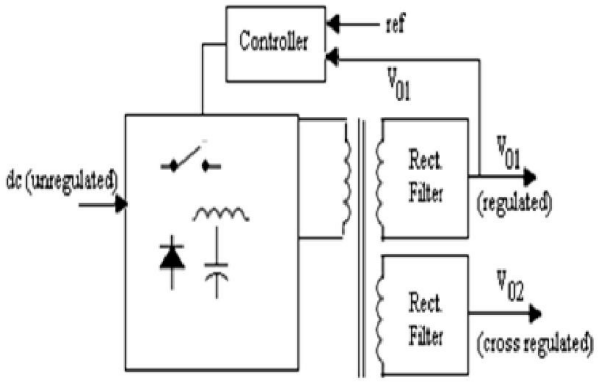

Fig. 1. *Multiple* outputs using single power converter

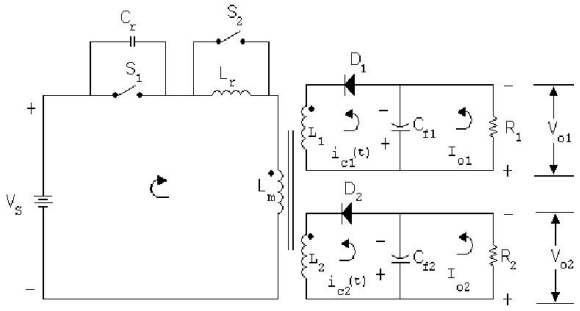

Fig. 2. Circuit diagram of multi-output flyback ZVS-QRC

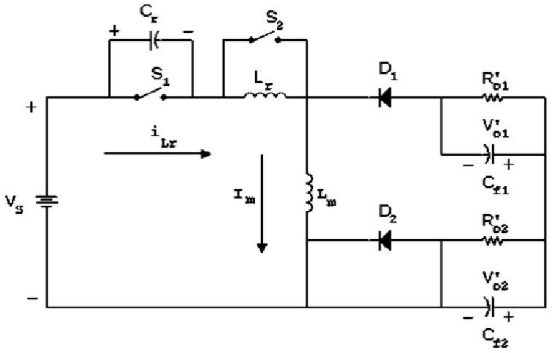

Fig. 3. Equivalent circuit diagram for the converter after transferring the elements from secondary to primary

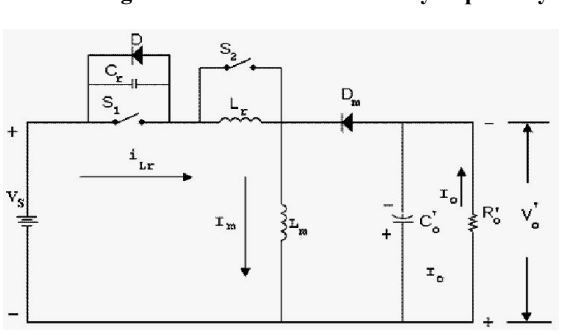

Fig. 4. Final equivalent circuit of the multi-output flyback ZVS-QRC

Normalized Load Resistance $R=\frac{R_O'}{Z_O}$

Voltage conversion ratio M_1 $= V_{o1} / V_s$

Voltage conversion ratio M_2 $= V_{o2} / V_s$

To simplify the analysis, the equivalent circuit diagram for the converter by transferring the elements from secondary to primary is shown in Fig. 3.Further modifications of Fig. 3 is shown in Fig. 4. Referring to Fig. 2 and Fig. 4, $V_0'=V_{oi}'$ and $V_{0i}=V_{oi}'$, where i =1, 2.Whenever a switching device changes from one state to another, the circuit configuration changes. Each configuration is referred to as a stage. In this QRC, six different stages are identified for each switching cycle and they are discussed as follows:

Linear capacitor charging stage (t_o, t_1)

The switch S_1 is opened to begin a new cycle at t = t_o. During this stage, the primary current I_m flows through the resonant capacitor C_r and its voltage increases linearly from zero to (V_s+V_o'). The capacitor voltage V_{cr} is governed by the equation

$$V_{cr}(t)=\frac{I_m t}{C_r} \tag{1}$$

When capacitor voltage $V_{cr}(t)$ reaches (V_s+V_o') at t = t_1, the diode D_m gets forward biased. The duration of this stage is given by

$$T_{d1}=t_1-t_2=\frac{C_r(V_s+V_o')}{I_m} \tag{2}$$

Resonant inductor discharging stage (t_1, t_2)

Stage 2 begins when the diode D_m conducts. The elements L_r and C_r form a series resonant circuit. The state equations are

$$\frac{dV_{cr}}{dt}=\frac{i_{Lr}(t)}{C_r}$$

$$\frac{di_{Lr}}{dt}=\frac{(V_s+V_o')-V_{cr}(t)}{L_r} \tag{3}$$

With initial conditions $V_{cr}(0)=(V_s+V_o')$ and $i_{Lr}(0)=I_m$. The solutions for the above equations are

$$\begin{aligned} V_{cr}(t) &= (V_s+V_o') + I_m Z_o \sin(\omega_o t) \\ i_{Lr}(t) &= I_m \cos(\omega_o t) \\ V_{Lr}(t) &= -I_m Z_o \sin(\omega_o t) \end{aligned} \tag{4}$$

At t_1, $i_{Lr}(t)$ reaches zero and $V_{cr}(t)$ reaches its peak value (refer Fig. 5) as

$$V_{cr}(t)=V_{cpeak}=(V_s+V_o')+I_m Z_o \tag{5}$$

When $V_{Lr}(t)$ reaches zero at t = t_2, the switch S_2 is turned ON to reduce losses as shown in Fig. 5. The duration of this stage is T_{d2} which is equal to $t_2 - t_1$.

$$T_{d2} = t_2 - t_1 = \frac{\pi}{\omega_o} \tag{6}$$

At t = t_2, the voltage across C_r then becomes $(V_S + V_o^{'})$

Holding stage (t_2, t_3)

This is the new stage, which characterizes the multi-output flyback ZVS-QRC. The constant switching frequency operation is achieved by introducing the holding stage, during which i_{Lr} and V_{cr} are held constant. The voltage V_{Lr} is clamped at zero value by keeping the switch S_2 closed. Then for this stage, voltage and current equations are given by

$$V_{cr}(t) = (V_S + V_o^{'})$$

$$i_{Lr}(t) = I_m \tag{7}$$

This stage continues until S_2 is turned OFF at t = t_3. The duration of this stage is T_{d3} which is equal to $t_3 - t_2$. The conversion ratio M_1 and M_2 can also be varied by varying T_{d3}.

Resonant inductor charging stage (t_3, t_4)

Resonance of L_r and C_r resumes when S_2 is turned OFF at t = t_3 and the corresponding equations are

$$\frac{di_{Lr}}{dt} = \frac{(V_S + V_o^{'}) - V_{cr}(t)}{L_r}$$

$$\frac{dV_{cr}}{dt} = \frac{i_{Lr}(t)}{C_r} \tag{8}$$

With initial conditions $V_{cr}(0) = (V_S + V_o^{'})$ and $i_{Lr}(0) = -I_m$ .The solutions for the above equations are

$$i_{Lr}(t) = I_m \cos(\omega_o t)$$

$$V_{cr}(t) = (V_S + V_o^{'}) - I_m Z_o \sin(\omega_o t) \tag{9}$$

This stage terminates when $V_{cr}(t)$ becomes zero. The duration of this stage is Td_4 which is equal to $t_4 - t_3$.

$$T_{d4} = \frac{1}{\omega_o}\arcsin\left(\frac{V_S + V_o^{'}}{I_m Z_o}\right) \qquad T_{d4} = \frac{(\alpha - \pi)}{\omega_o}$$

$$\alpha = \pi + \arcsin\left(\frac{V_S + V_o^{'}}{I_m Z_o}\right) \tag{10}$$

where α lies in the range $\pi < \alpha < 3\pi / 2$. Then the inductor current i_{Lr} is given by the equation

$i_{Lr}(t_4) = I_m \cos(\alpha)$.

Linear inductor charging stage (t_4, t_5)

The switch S_1 is turned ON at t=t_4 as shown in Fig. 5, when V_{cr} becomes zero to reduce turn-on loss. The current i_{Lr} increases linearly and reaches I_m at t = t_5. Beyond t_4, the capacitor voltage is clamped to zero by the diode D as shown in Fig. 4. The corresponding state equation is

$$\frac{di_{Lr}}{dt} = \frac{V_S + V_o^{'}}{L_r} \tag{11}$$

With initial condition, $i_{Lr}(t)$ is given by

$$i_{Lr} = \left(\frac{V_S + V_o^{'}}{I_m Z_o}\right) + I_m \cos(\alpha) \tag{12}$$

This stage terminates when inductor current becomes I_m. The duration of this stage is given by

$$T_{d5} = \left(\frac{I_m Z_o (1 - \cos(\alpha))}{(V_S + V_o^{'})\omega_o}\right) \tag{13}$$

Constant current stage (t_5, t_6)

Once the inductor current $i_{Lr}(t)$ reaches I_m at t_5, the diode D_m turns OFF. The switch S_1 conducts as long as it is kept ON. At t_6, the switch S_1 is turned OFF which starts the new cycle. The duration of this stage is T_{d6} which is equal to $t_6 - t_5$. The theoretical waveforms of the multi-output flyback ZVS-QRC are shown in Fig. 5.

Open Loop Simulation

Design Procedure

The design parameter of a multi-output fly back ZVS-QRC (Arulselvi *et al*., 2005; Arulselvi, 2007), tabulated in Table I are used for analysis and simulation studies. Selecting normalized frequency, f_{ns} as 0.15 and the switching frequency f_s as 25 kHz, the resonant frequency is calculated as $f_o = f_s/0.15$ = 165 kHz. The condition for zero voltage switching is

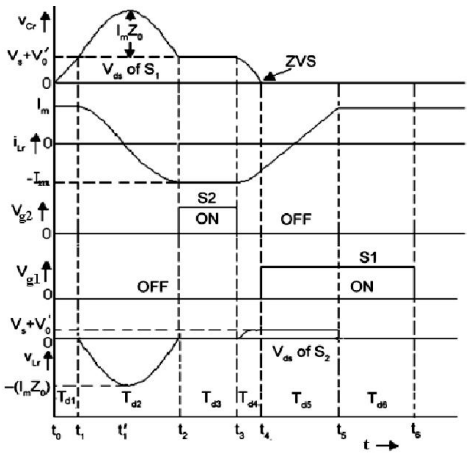

Fig. 5. Theoretical waveforms of multi-output flyback ZVS-QRC

Table 1. Design parameters

V_s (V)	V_{01} (V)	V_{02} (V)	I_{01} (A)	I_{02} (A)	L_r µH	C_r µF	f_s kHz	f_o kHz
12	5	12	1	0.5	28.2	0.0333	25	165

$$I_m Z_o > (V_S + V_o^{'}) \quad (14)$$

Maximum magnetizing current I_m at nominal load

$I_m = (M+1)I_o = 2.1A$

Where, $I_o = I_{o1}n_1 + I_{o2}n_2$ and $M = V_S / V_o^{'}$.

Therefore to satisfy(14), Z_o>12Ω, using Z_o and f_o values, the resonant components L_r and C_r are calculated as 28.2µH and 0.0333µF, respectively.

Open loop simulation results

The open loop simulation of multi-output fly back ZVS-QRC is carried out using MATLAB/SIMULINK software. The simulated resonant capacitor voltage (V_{cr}), resonant inductor current(i_{Lr}) and gate pulses applied to S_1(V_{g1}) and S_2 (V_{g2}) for the nominal load conditions of secondary are shown in Fig. 6. It is seen that these waveforms agree closely with the theoretical waveforms as shown in Fig. 5. It is observed from Fig. 7and 8 that in open loop operation, the converter output deviates from the required output voltage 5V and 12V and settles at a new value after a sudden load current changes at time t = 9 msec from 1A to 1.42A. Hence a closed loop control is needed to regulate the output voltages against load variation.

Closed Loop Simulation

The block diagram of closed - loop control is shown in Fig.9. To regulate the output voltage V_{o1}, the switching frequency of the PWM pulses are varied depends on error. Since output V_{01} is very sensitive to load variation by producing large deviations from nominal value for small variations in load. Hence a closed-loop control is designed to maintain tight regulation of V_{01} against load variation and V_{02} is cross-regulated.

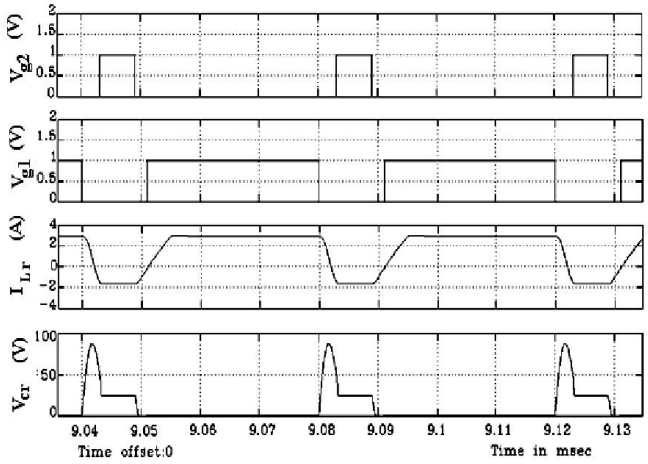

Fig. 6. Simulated waveforms showing the gate pulse of the switches, resonant inductor current, and resonant capacitor voltage

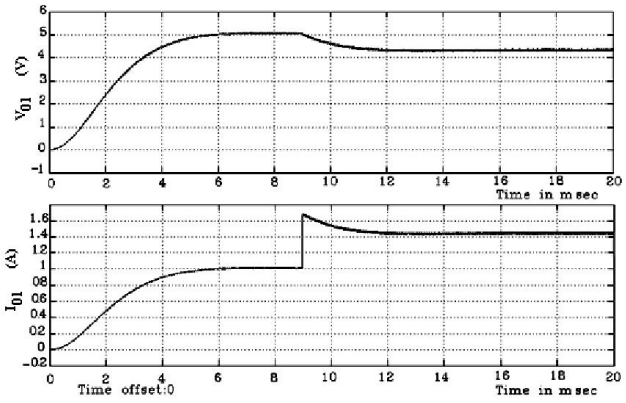

Fig. 7. Output voltage (V_{01}) and current (I_{01}) of secondary 1 for sudden load current (I_{01}) variation of 1A to 1.4A

Closed-loop control using conventional fuzzy logic control (CFLC)

The inputs to the CFLC are the error voltage (e) and change in error (ce). The output is the change in switching frequency (Δu). Depending on the magnitude and sign of e and ce, the switching frequency of the main switch S_1 and auxiliary switch S_2 is varied to regulate the output voltage. For ease of computation, the variables e, ce and Δu are divided into five fuzzy subsets using triangular membership function as shown in Fig.10. Regulated output voltages V_{o1} and I_{o1} for sudden increase in load current (I_{o1}) at time t = 9msec from 1A to 0.7A are shown in Fig.11. The performances of FLC are given in Table 4.

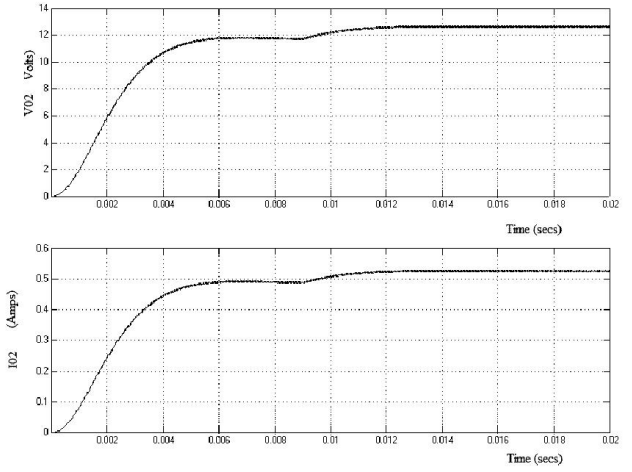

Fig. 8. Output voltages V_{02} and I_{02} of secondary2 for sudden load current (I_{01}) variation of 1A to 1.4A

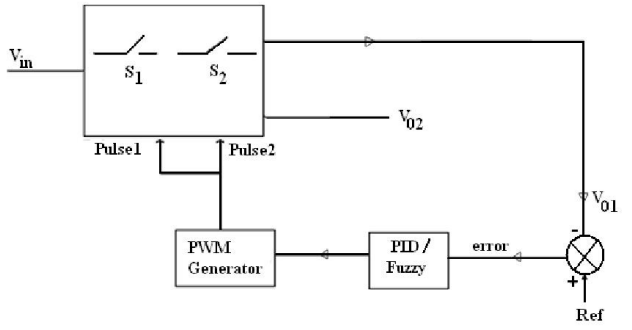

Fig. 9. Block diagram of closed loop control of multi-output ZVS flyback QRC

Closed-loop control using SFLC

The SFLC is designed for CFLCs with skew symmetric property similar to Table 2, most rule tables used in power converters applications have skew property, i.e. the output membership values along the leading diagonal of the rule table are zero-valued and those on either side of this diagonal take opposite signs $\Delta uij = -\Delta uji$ where Δuij is the output membership function along the *i*th the row and *j*th column. Also, the magnitude of the control signal is approximately equal to the distance from the main diagonal line or switching line (*ds*) of the rule table as shown in Fig. 12. For a general second order system, the switching line is given in eqn (15). For the present case, switching line has unity slope passing through origin and it is defined as given in eqn (16). This property is utilized to suggest a new variable called signed distance (*ds*), which is declared as the shortest distance between switching line and the present operating point. From any operating point, the control variable is directly related to the signed distance (*ds*), which is the input variable to the SFLC. The output of SFLC is considered as change of switching frequency (Δu). As a result, the number of fuzzy rules required becomes minimum and the firing rule table is reduced to one-dimensional space compared to CFLC.

The equation for switching line is

$$ce + \lambda e = 0 \quad (15)$$

For $\lambda = 1$, $ce + e = 0$ (16)

The intersection point *H* (*e*, *ce*) of the switching line from an operating point *P*(*e*1, *ce*1) is illustrated in Fig. 9. The distance *ds* between *H*(*e*, *ce*) and *P*(*e*1, *ce*1) for a general point *P*(*e*, *ce*) is expressed as given in eqn (21) for a second-order system and is deduced to eqn (22) for the present case.

$$ds=sgn(y)*((|ce+\lambda e|) / 1+\lambda 2) \quad (17)$$

$$ds=sgn(y)*((|ce+e|) / 2) \quad (18)$$

$$sgn(y) = \quad f(x) = \begin{cases} 1, & y > 0 \\ -1, & y < 0 \end{cases}$$

and $y = ce + e$ (20)

The sign of the control signal (Δu) for ZVS-QRC, is positive for $y > 0$ and negative for $y < 0$ and its absolute magnitude is proportional to the distance from the switching line. Triangular membership functions with the five linguistic values are designed for *ds* and Δu. The range of *ds* and Δu are also normalized to [–1 1] and the membership diagram is shown in Fig. 14. The fuzzy rule for SFLC is constructed between the signed distance *ds a*nd the control variable Δu as shown in Table 3. The inference mechanism, defuzzification and denormalization are carried out in a manner similar to CFLC.

Table 2. Fuzzy Rule Base

ce \ e	NB	NS	Z	PS	PB
NB	NB	NB	NS	NS	Z
NS	NB	NS	NS	Z	PS
Z	NS	Z	Z	PS	PB
PS	NS	Z	PS	PB	PB
PB	Z	PS	PB	PB	PB

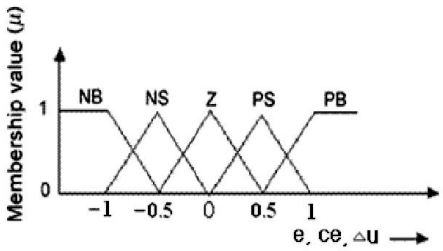

Fig. 10. Membership function diagram of c, ce, Δu

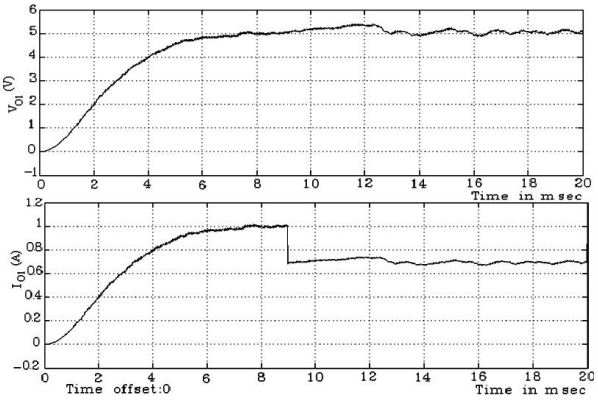

Fig. 11. Regulated output voltage (V_{o1}) and current (I_{o1}) of secondary1 for sudden load current (I_{o1}) variation of 1A to 0.7 A with FLC

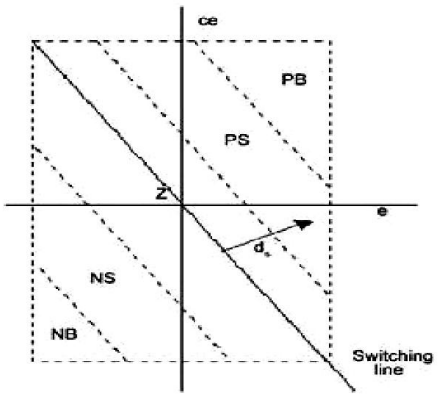

Fig.12. Simplified plot of CFLC rule table

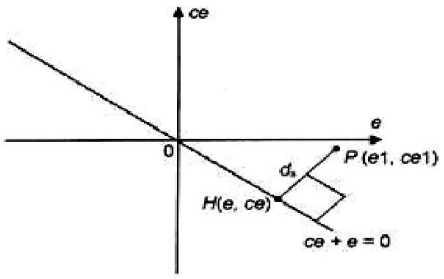

Fig. 13. Plot showing calculation of signed distance (d_s) for ZVS-QRC

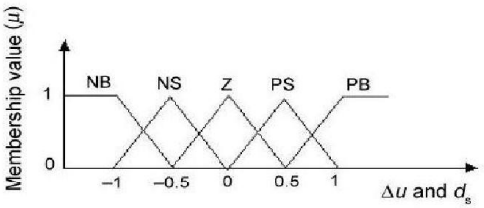

Fig. 14. Membership function diagram of d_s and Δu.

Table 3. Control rules for SFLC

d_s	PB	PS	Z	NS	NB
Δu	PB	PS	Z	NS	NB

This method can be extended to CFLC design based on *n* inputs. In this case, the rule table is established on *n*-dimensional space of *e*1, *e*2… *en*. The number of rules for *m*-fuzzy sets becomes *mn*, which makes it very difficult to generate reasonable control rules. Similar to two-dimensional rule table, *n*-dimensional table also satisfies the skew-symmetric and the absolute magnitude of the control input is proportional to the distance from its main diagonal of hyper plane. The switching hyper plane is

$$e^{(n-1)} + \gamma_{n-1}e^{(n-2)} + \ \ldots + \gamma_2\dot{e} + \gamma_1 e = 0$$

Then signed distance d_s from the operating point to the switching hyper plane of eqn (25) can be calculated as

$$d_s = \frac{e^{(n-1)} + \gamma_{n-1}e^{(n-2)} + \ \ldots + \gamma_2\dot{e} + \gamma_1 e}{\sqrt{1 + \gamma_{n-1}^2 + \cdots + \gamma_2^2 + \gamma_1^2}}$$

Then the rule table is established equivalent to Table 2. This makes SFLC very simple.

Table 4. Performance Measures

	Fuzzy logic controller		Single input Fuzzy logic controller	
	Up load	Down load	Up load	Down load
ISE	0.04546	0.04473	0.04429	0.04415
T_r(sec)	0.0063	0.0058	0.0072	0.006
Offset(V)	0.17	0.076	0.14	0.056
T_s(msec)	17	17.5	13.5	15

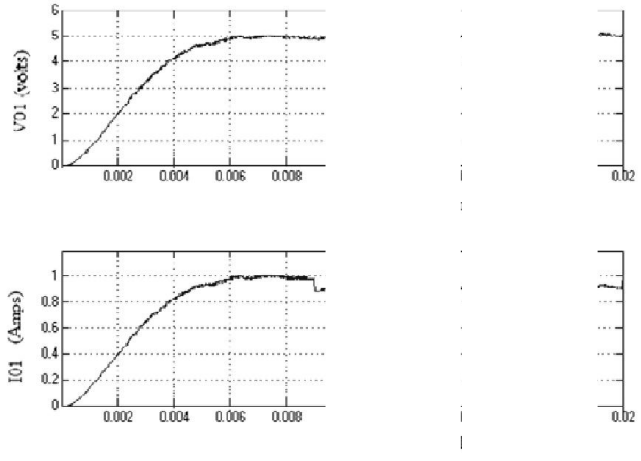

Fig. 15. Regulated output voltage (V_{o1}) and current (I_{o1}) of secondary1 for sudden load current (I_{o1}) variation of 1A to 0.7A with SFLC

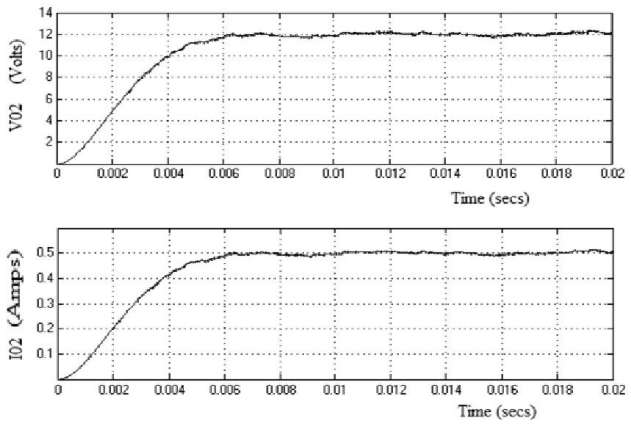

Fig. 16. Regulated output voltage (V_{o2}) and current (I_{o2}) of secondary2 for sudden load current (I_{o1}) variation of 1A to 0.7A with SFLC

Conclusion

The performances of the multi output flyback converter with conventional PI controller and fuzzy logic controller are compared. The ISE value, rise time(T_r), settling time(T_s) and offset for sudden load current increase from 1A to 1.42A and sudden load current decrease from 1A to 0.7A are tabulated in Table IV. It can be concluded that Single input fuzzy logic controller is a better choice than conventional Fuzzy logic controller in terms of less ISE and offset.

REFERENCES

Baha, B. "Analysis and control of a cross-regulated multi-output forward quasi-resonant converter," *IEEE Proc.-Circuits Devices Syst.,* vol. 146*,* no. 5, pp. 255-262,October 1999.

Issa Batarseh, *Power Electronic Circuits*, John Wiley and Sons, 2004.

Dananjayan, P., V. Sriram, C. Chellamithu. "A flyback constant frequency ZCS-ZVS quasi-resonant converter," *Elsevier Microelectronics journal,* vol 29, pp.495-504,1998.

Jai P. Agarwal, "Determination of cross regulation in multi-output resonant converters," *IEEE Transl. on Aerospace and electronic system.,* vol. 36*,* no. 3,pp. 760-772,July 2000.

Arulselvi, S., K. Deepa, G. Uma. "Design, analysis and control of a new multi-output flyback CF-ZVS-QRC," *in Proc. IEEE/ICIT Conf*, Hongkong,pp.413-419,December-2005.

Arulselvi, S. "Conventional and intelligent control of hard-switched and soft-switched dc-dc converters," Ph.D. dissertation, Anna Univ., Chennai,India,2007.

Balu Balakrishnan, *Data Book and Design Guide*. Power Integrations, U.S.A,2005.

George Stephanopoulos,Chemical Process Control,Prentice Hall of India,1994.

****